

In-place implementation of Quantum-Gimli

Lars Schlieper* 

Horst Görtz Institute for IT Security
Ruhr University Bochum, Germany
{lars.schlieper}@rub.de

Abstract. We present an in-place implementation of the cryptographic permutation GIMLI, a NIST round 2 candidate for lightweight cryptography, and provide an upper bound for the required quantum resource in depth and gate-counts. In particular, we do not use any ancilla qubits and the state that our circuit produces is not entangled with any input. This offers further freedom in the usability and allows for a widespread use in different applications in a plug-and-play manner.

Keywords: Quantum Algorithm, Implementation, Permutation, GIMLI, In-Place, Circuit, Reducing/Minimize Qubits.

1 Introduction

In recent years, the realization of quantum computers has made great progress [13]. With the launch of the NIST post quantum competition quantum computers have moved even more into the focus of security considerations. One of the subjects being considered in research is the limits of quantum attacks on existing cryptosystems. Recently there have been many results concerning Grover attacks on symmetric ciphers, especially on lightweight ciphers. This includes related implementations and resource estimates of the quantum implementation of the ciphers and attacks [2,5,7,8,12], as well as attempts to adapt classical attacks into the quantum setting [6,10,11,16]. These approaches have in common that they require an (efficient) quantum implementation of the targeted cipher.

Another reason for such implementations is the connection of quantum computers to a kind of quantum internet [4,14] and the resulting necessity of encryption procedures. These have to be either efficient implementations of classical encryption schemes or even own quantum encryption schemes which may exploit entanglements.

For many such ciphers permutations are required. These can be implemented in various ways. Two of these possibilities are either as a lookup table or directly as a circuit. The approach to realize these permutations in a quantum setting by a lookup table is problematic, because for a superposition request to the permutation the table must also allow for an efficient superposition request.

* Funded by DFG under Germany's Excellence Strategy - EXC 2092 CASA - 390781972.

On the other hand, the circuit approach requires an embedding, which has the advantage that permutations are already reversible.

Apart from the standard reversible embedding of n -bit to n -bit functions with at least $2n$ bits [15], Vivek V. et al showed in [17] that any permutation can be implemented with a maximum of $n + 1$ bits over the CNT-gate-set (CNOT, NOT, CCNOT), but not necessarily efficiently, namely with polynomial depth and a polynomial number of gates.

The number of possible permutations alone shows that an efficient implementation over this gate-set is not possible for every permutation. This raises the question which permutations can be efficiently implemented.

We show in this paper that GIMLI [3] is an efficient implementable permutation. Further more we show that even an in-place implementation is possible. Therefore the permutation of superpositions is possible without entanglement with "input bits".

Our contributions: To the best of our knowledge we give the first step-by-step reversible in-space implementation of the GIMLI-permutation [3] in QISKIT [1], which is provided by IBM. In addition, we give in this case study a polynomial upper-bound for the number of required gates, depth, depending on the number of rounds and the word lengths of GIMLI.

Our circuit can be used as a building block or starting point for further applications and research. In particular, since there is no entanglement between input and output, this may open up further possibilities.

Furthermore, the realization of GIMLI as a quantum circuit out of reversible gates directly provides a circuit for the inverse of GIMLI.

Organization: In Section 2 we first introduce the notation and model we use. In Section 3 we briefly recall the original GIMLI-permutation. In Section 4 we then build our implementation of the quantum circuit step by step and specify the circuit size.

2 Preliminaries

Let us first recall some notations. For the classical part we use the same notation as in the original GIMLI paper [3]. We define $\mathcal{W} := \{0, 1\}^{32}$ and use

- $a \oplus b$ to denote a bitwise **exclusive or** (XOR) of the values a and b ,
- $a \wedge b$ for a bitwise logical **and** of the values a and b ,
- $a \vee b$ for a bitwise logical **or** of the values a and b ,
- $a \lll k$ for a **cyclic left shift** of the value a by a shift distance of k , and
- $a \ll k$ for a **non-cyclic shift** (i.e, a shift that is filling up with zero bits) of the value a by a shift distance of k .

Further we describe our words $w \in \mathcal{W}$ as vectors $w = (w_0, \dots, w_{31})$. We refer to a 384-bit state as a $3 \times 4 \times 32$ -matrix over $\{0, 1\}$, or equivalently as a 3×4 matrix over words $s_{i,j} \in \mathcal{W}$. The quantum gates used in this paper can be derived from

the Clifford+ T set and are the NOT gate X , Hadamard-gate H , Phase shift gates T, T^\dagger to the angles $\frac{\pi}{4}, \frac{-\pi}{4}$,

$$X := \begin{pmatrix} 0 & 1 \\ 1 & 0 \end{pmatrix}, \quad H := \frac{1}{\sqrt{2}} \begin{pmatrix} 1 & 1 \\ 1 & -1 \end{pmatrix}, \quad T := \begin{pmatrix} 1 & 0 \\ 0 & \frac{1+i}{\sqrt{2}} \end{pmatrix}, \quad T^\dagger := \begin{pmatrix} 1 & 0 \\ 0 & \frac{1-i}{\sqrt{2}} \end{pmatrix}$$

as well as the multi-qubit gates CNOT (controlled NOT) and CCNOT (Toffoli),

$$\text{CNOT} := \begin{pmatrix} 1 & 0 & 0 & 0 \\ 0 & 1 & 0 & 0 \\ 0 & 0 & 0 & 1 \\ 0 & 0 & 1 & 0 \end{pmatrix} \sim \begin{array}{c} \bullet \\ | \\ \oplus \end{array}, \quad \text{CCNOT} := \begin{pmatrix} 1 & 0 & 0 & 0 & 0 & 0 & 0 & 0 \\ 0 & 1 & 0 & 0 & 0 & 0 & 0 & 0 \\ 0 & 0 & 1 & 0 & 0 & 0 & 0 & 0 \\ 0 & 0 & 0 & 1 & 0 & 0 & 0 & 0 \\ 0 & 0 & 0 & 0 & 1 & 0 & 0 & 0 \\ 0 & 0 & 0 & 0 & 0 & 1 & 0 & 0 \\ 0 & 0 & 0 & 0 & 0 & 0 & 1 & 0 \\ 0 & 0 & 0 & 0 & 0 & 0 & 0 & 1 \end{pmatrix} \sim \begin{array}{c} \bullet \\ | \\ \bullet \\ | \\ \oplus \end{array},$$

which can be constructed in-place with the gate above, as seen in Figure 1.

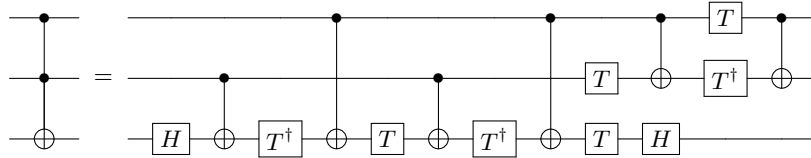


Fig. 1: In-place implementation of Toffoli via H, T, T^\dagger and CNOT-gates.

Further we use the SWAP-operation,

$$\text{SWAP} := \begin{pmatrix} 1 & 0 & 0 & 0 \\ 0 & 0 & 1 & 0 \\ 0 & 1 & 0 & 0 \\ 0 & 0 & 0 & 1 \end{pmatrix} \sim \begin{array}{c} \times \\ | \\ \times \end{array} \sim \begin{array}{c} \bullet \\ | \\ \oplus \\ | \\ \oplus \\ | \\ \bullet \end{array} \sim \begin{array}{c} \times \\ | \\ \times \end{array}.$$

We consider in this paper quantum-circuits over the set of gates above, under the standard assumptions of full-parallelism, full-connectivity and we do not consider errors. Associated with this we do not count SWAP-operations and take them as free, instead we will re-label the qubits accordingly as in [8].

3 Gimli

GIMLI [3] is a 384-bit permutation, candidate of the second round of NIST's lightweight cryptography competition and designed to achieve high security with high performance across a broad range of platforms. This cryptographic primitive is suitable for many different applications, e.g. collision-resistant hashing, preimage-resistant hashing, message authentication, and message encryption.

Let us briefly recall GIMLI (Algorithm 1). It is a round-based permutation on a 384-bit state $s = (s_{i,j}) \in \mathcal{W}^{3 \times 4}$. Each of the 24 rounds is a sequence of at most three operations:

- a non-linear layer, where a 96-bit SP-Box is applied to each column;
- in every second round, a linear mixing layer;
- in every fourth round, an addition of a constant and the round-number.

Algorithm 1: GIMLI

Input : $s = (s_{i,j}) \in \mathcal{W}^{3 \times 4}$
Output: $\text{GIMLI}(s) \in \mathcal{W}^{3 \times 4}$

```

1 begin
2   for  $r$  from 24 downto 1 inclusive do
3     for  $j$  from 0 to 3 inclusive do ▷ SP-Box
4        $x \leftarrow s_{0,j} \lll 24$ 
5        $y \leftarrow s_{1,j} \lll 9$ 
6        $z \leftarrow s_{2,j}$ 
7        $s_{2,j} \leftarrow x \oplus (z \lll 1) \oplus ((y \wedge z) \lll 2)$ 
8        $s_{1,j} \leftarrow x \oplus y \oplus ((x \vee z) \lll 1)$ 
9        $s_{0,j} \leftarrow y \oplus z \oplus ((x \wedge y) \lll 3)$ 
10    end
11    if  $r \equiv 0 \pmod{4}$  then ▷ Small-Swap
12       $s_{0,0}s_{0,1}s_{0,2}s_{0,3} \leftarrow s_{0,1}s_{0,0}s_{0,3}s_{0,2}$ 
13    end
14    if  $r \equiv 2 \pmod{4}$  then ▷ Big-Swap
15       $s_{0,0}s_{0,1}s_{0,2}s_{0,3} \leftarrow s_{0,2}s_{0,3}s_{0,0}s_{0,1}$ 
16    end
17    if  $r \equiv 0 \pmod{4}$  then ▷ Add constant
18       $s_{0,0} \leftarrow s_{0,0} \oplus c \oplus r$ 
19    end
20  end
21  return  $s$ 
22 end
```

Remark 3.1. GIMLI appears to be easily scalable in the number of rounds r and the length ℓ of the words s in \mathcal{W} , where scaling may affect the security.

4 Quantum Gimli

In this section we give the description of our in-place quantum circuit for the GIMLI permutation. Let us begin by subdividing GIMLI into even smaller pieces.

The linear parts of GIMLI are two different SWAP operations, called SMALL-SWAP and BIG-SWAP, and a XOR with a constant and the round-number. Samuel Jaques et al. describe in [9] how every invertible linear function can be implemented efficiently in-place by using the numerical procedure of PLU decomposition. In case of the linear functions of GIMLI it is even easier to implement them. The XOR with a constant and the round-number can be hard-wired at the necessary points via NOT-gates, since they are known in advance. The two different SWAP operations can either be implemented by SWAP-gates or by relabelling. While using the relabelling technique we have to pay attention to the new labels of the qubits and so we have to be careful to use the correct bits in the further calculation. The underlying bit-permutation can be easily calculated and can be created with the algorithm in the supplementary material. At the end either the new labels have to be taken into account for further computations or we have to add a SWAP-layer to swap the qubits via SWAP-gates back in the correct order.

The non-linear part of GIMLI, the SP-BOX, is a bit more tricky. The SP-BOX works on three inputs words $x, y, z \in \mathcal{W}$ (96-bits) and can again be split into three parts:

1. a cyclic shift of x and y by 24 and 9

$$\begin{aligned} x &\leftarrow x \lll 24 \\ y &\leftarrow y \lll 9. \end{aligned}$$

2. three parallel updates of x, y and z via a T-function with non-cyclic shifts as part of the calculation

$$x \leftarrow x \oplus (z \ll 1) \oplus ((y \wedge z) \ll 2) \tag{1}$$

$$y \leftarrow x \oplus y \oplus ((x \vee z) \ll 1) \tag{2}$$

$$z \leftarrow y \oplus z \oplus ((x \wedge y) \ll 3). \tag{3}$$

3. a Swap of x and z

$$\begin{aligned} x &\leftarrow z \\ z &\leftarrow x. \end{aligned}$$

The parts 1 and 3 can also be done by relabelling similar to the SWAPs. It remains to show how part 2 (the T-function) can be efficiently implemented in-place. First we notice that to achieve an in-place implementation we can **not** simply use the "classic" universal embedding of the T-function, update x, y and z as in GIMLI via an additional register, nor calculate x, y and z one after the other, since they are dependent on each others non-updated value and we do **not** want to use extra space for this calculations.

We instead use a bitwise approach and exploit the fact, that for each bit x_k, y_k and z_k of x, y and z no bits with a lower index are used to calculate the update and that by a non-cyclic shift the vector is refilled with zeros. We hence compute x, y and z bit by bit in such an order that the updated bits are no longer necessary for further updates of other bits. To make our approach more precise, let us first take a look at the update of the individual bits of x, y and z in Equations (1), (2) and (3). The individual bits are computed as

$$x_k \leftarrow x_k \oplus z_{k+1} \oplus (y_{k+2} \cdot z_{k+2}) \quad (4)$$

$$y_k \leftarrow x_k \oplus y_k \oplus ((x_{k+1} \oplus 1) \cdot (z_{k+1} \oplus 1)) \oplus 1 \quad (5)$$

$$z_k \leftarrow y_k \oplus z_k \oplus (x_{k+3} \cdot y_{k+3}), \quad (6)$$

where we used De Morgan's laws with $A \vee B = \overline{\overline{A} \wedge \overline{B}}$ for the computation of y_k and define $(x_j, y_j, z_j) = (0, 0, 0)$ for $j > 31$. If we can compute x_k, y_k and z_k "parallel" without use of any ancilla bits now, we can compute x, y and z inductively from $k = 0$ to $k = 31$ in-place. Indeed, this can be done by the circuit seen in Figure 2, where x'_k, y'_k and z'_k represent the updated x_k, y_k and z_k as shown in Equations (4), (5) and (6).

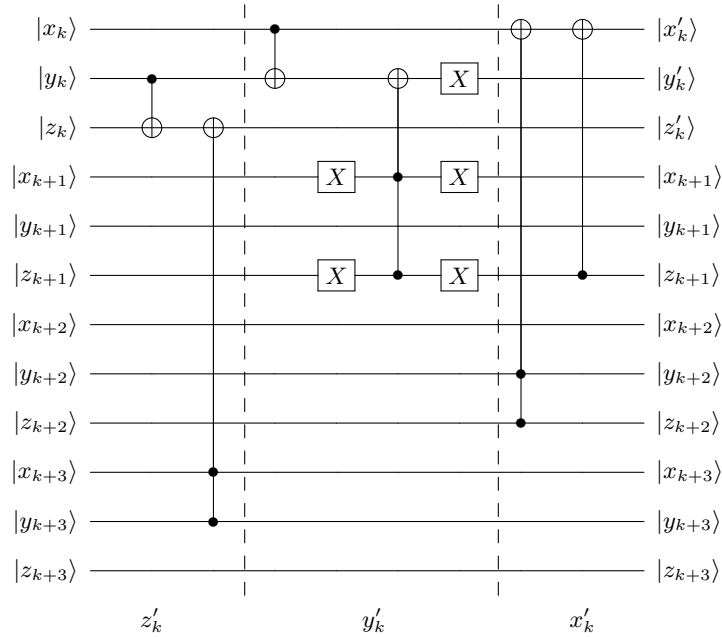


Fig. 2: Circuit for updating x_k, y_k and z_k "parallel" in depth 5 (T_k -function). With $(x_k, y_k, z_k) = (0, 0, 0)$ for $k \geq 32$.

For $k \geq 29$ the CNOTs and CCNOTs with missing control-bits are adjusted. For $k = 31$ the NOT on y_k is omitted, since it would be cancelled with the CCNOT only controlled with ones. From here on we can build up the whole circuit of our GIMLI in-place implementation. First we get the full T-function as seen in Figure 3.

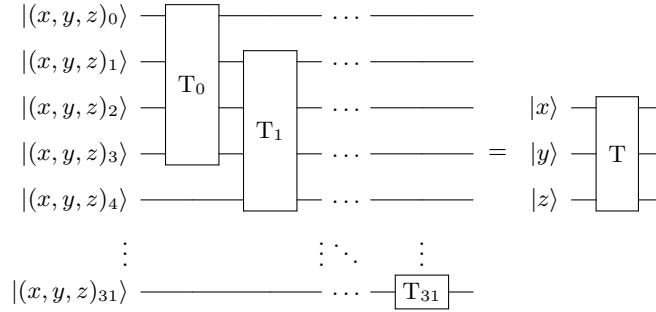


Fig. 3: T Circuit.

With this we can build the SP-BOX as seen in Figure 4.

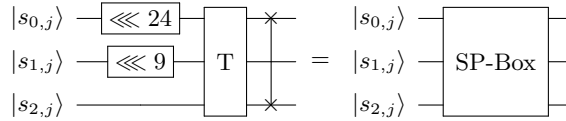


Fig. 4: Non-linear layer (SP-Box).

The SP-BOX together with the discussion above, regarding the linear layers, directly leads to the whole circuit where the circuit-part seen in Figure 5 is repeated 6 times for 24 rounds. The whole circuit can also be build using algorithm 2. A python implementation with QISKIT of algorithm 2 can be found in the supplementary material.

Remark 4.1. Related to the variables of rounds r and word length ℓ the depth of the circuit is upper-bounded by $5 \cdot \ell \cdot r + \frac{r}{4}$. Here the 5 comes from the depth of T_k (Figure 2) and the $\frac{r}{4}$ from the XOR of the key.

The depth of this circuit for the given parameter $l = 32$ and $r = 24$ is upper bounded by 3846, whereas (by shifting parts of the circuit into each other) the circuit produced by algorithm 2 has only a depth of 3104. This can be further reduced by employing more qubits instead of operating only on the 384 input qubits.

The limitation on 384 qubits also means that we get the output of the permutation without use of ancilla qubits and entanglement with the input, as would be the case with the "classic" universal embedding, which can provide additional freedom for further use.

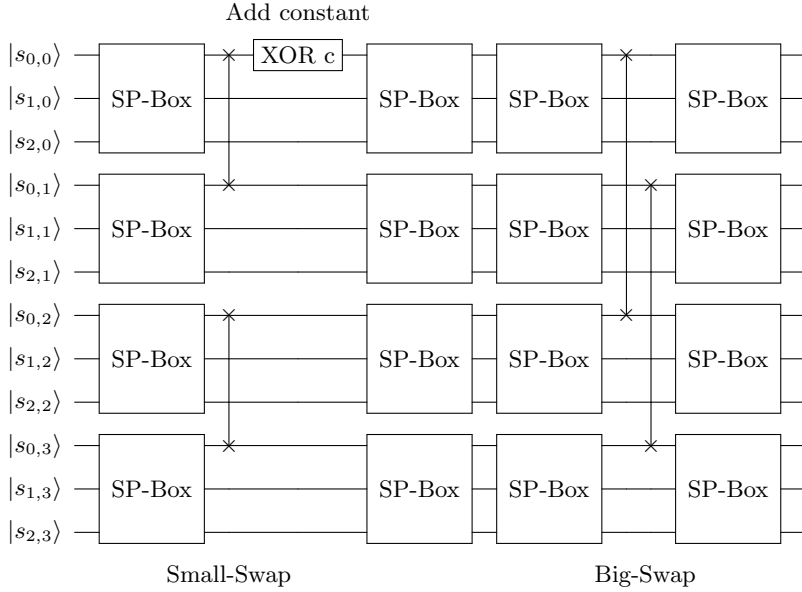


Fig. 5: 4 of 24 Rounds of the GIMLI-circuit.

4.1 Properties

In the following we list the depth and gate numbers of the circuit generated by algorithm 2. Here we give the values for a circuit generated with CCNOTs, as well as the values for the circuit where the CCNOTs are replaced with the construction from Figure 1. Since the T, T^\dagger gates are considered to be the gates with the highest error, we additionally specify the depth of the T, T^\dagger gates for the circuit with replaced CCNOTs. The results can be seen in Table 1, and are optimal in the sense that the internal optimizer of QISKIT is not able to improve them.

Circuit	Depth	Gatecount	X	CCNOT	CNOT	H	T	T -depth
With CCNOTs	3104	32739	14979	8640	9120	0	0	0
Without CCNOTs	14908	153699	14979	0	60960	17280	60480	168

Table 1: Depths and gate numbers of the circuit generated by algorithm 2. T and T^\dagger gates are summarized in this table.

Remark 4.2. For varying number of rounds r and word length ℓ the depths and gate numbers increase linearly in r, ℓ .

For further verification we have programmed a classic 1:1 version of the generated circuitry and let it compete with random input against the original python implementation, which produced the same results as GIMLI in our 1.000.000 test. The original implementation of GIMLI and the classic version of the circuit can also be found in the supplementary material.

Algorithm 2: Quantum-GIMLI circuit builder.

Output: Quantum circuit Q_{GIMLI} , qubit label dictionary L

```
1 begin
2   Define empty quantum circuit  $Q_{\text{GIMLI}}$  with 384 qubits.
3   Define  $L = (s_{i,j})_{0 \leq i < 3, 0 \leq j < 4}$  as label dictionary.
4   for  $r$  from 24 downto 1 inclusive do
5     for  $j$  from 0 to 3 inclusive do ▷ SP-Box
6       Relabel qubit registers/update  $L$  correspondingly
7        $s_{0,j} \lll 24$  and  $s_{1,j} \lll 9$ .
8       for  $k$  from 0 to 31 inclusive do ▷  $T_k$ 
9         Add circuit from Figure 2 correspondingly  $j, k$  and  $L$ 
10        with  $x \sim s_{0,j}, y \sim s_{1,j}$  and  $z \sim s_{2,j}$ .
11      end
12      Relabel qubit registers/update  $L$  correspondingly
13       $s_{0,j}s_{1,j}s_{2,j} \leftarrow s_{2,j}s_{1,j}s_{0,j}$ .
14    end
15    if  $r \equiv 0 \pmod{4}$  then ▷ Small-Swap
16      Relabel qubit registers/update  $L$  correspondingly
17       $s_{0,0}s_{0,1}s_{0,2}s_{0,3} \leftarrow s_{0,1}s_{0,0}s_{0,3}s_{0,2}$ .
18    end
19    if  $r \equiv 2 \pmod{4}$  then ▷ Big-Swap
20      Relabel qubit registers/update  $L$  correspondingly
21       $s_{0,0}s_{0,1}s_{0,2}s_{0,3} \leftarrow s_{0,2}s_{0,3}s_{0,0}s_{0,1}$ .
22    end
23    if  $r \equiv 0 \pmod{4}$  then ▷ Add constant
24      Add NOT gates related to  $\text{bin}(c)$ ,  $\text{bin}(r)$  and  $L$ .
25    end
26  end
27 return  $Q_{\text{GIMLI}}, L$ .
28 end
```

References

1. Qiskit: An open-source framework for quantum computing, 2019. doi:10.5281/zenodo.2562110.
2. Ravi Anand, Arpita Maitra, and Sourav Mukhopadhyay. Grover on simon, 2020.
3. Daniel J. Bernstein, Stefan Kölbl, Stefan Lucks, Pedro Maat Costa Massolino, Florian Mendel, Kashif Nawaz, Tobias Schneider, Peter Schwabe, François-Xavier Standaert, Yosuke Todo, and Benoît Viguier. Gimli : A cross-platform permutation. In Wieland Fischer and Naofumi Homma, editors, *Cryptographic Hardware and Embedded Systems – CHES 2017*, pages 299–320, Cham, 2017. Springer International Publishing.
4. Marcello Caleffi, Daryus Chandra, Daniele Cuomo, Shima Hassanpour, and Angela Sara Cacciapuoti. The rise of the quantum internet. *IEEE Computer*, 53(6):67–72, 2020. doi:10.1109/MC.2020.2984871.

5. Markus Grassl, Brandon Langenberg, Martin Roetteler, and Rainer Steinwandt. Applying grover’s algorithm to AES: quantum resource estimates. In Tsuyoshi Takagi, editor, *Post-Quantum Cryptography - 7th International Workshop, PQCrypto 2016, Fukuoka, Japan, February 24-26, 2016, Proceedings*, volume 9606 of *Lecture Notes in Computer Science*, pages 29–43. Springer, 2016. doi:10.1007/978-3-319-29360-8_3.
6. Akinori Hosoyamada and Yu Sasaki. Cryptanalysis against symmetric-key schemes with online classical queries and offline quantum computations. In Nigel P. Smart, editor, *Topics in Cryptology - CT-RSA 2018 - The Cryptographers’ Track at the RSA Conference 2018, San Francisco, CA, USA, April 16-20, 2018, Proceedings*, volume 10808 of *Lecture Notes in Computer Science*, pages 198–218. Springer, 2018. doi:10.1007/978-3-319-76953-0_11.
7. Kyungbae Jang, Seungjoo Choi, Hyeokdong Kwon, and Hwajeong Seo. Grover on speck: Quantum resource estimates, 2020.
8. Samuel Jaques, Michael Naehrig, Martin Roetteler, and Fernando Virdia. Implementing grover oracles for quantum key search on AES and lowmc. In Anne Canteaut and Yuval Ishai, editors, *Advances in Cryptology - EUROCRYPT 2020 - 39th Annual International Conference on the Theory and Applications of Cryptographic Techniques, Zagreb, Croatia, May 10-14, 2020, Proceedings, Part II*, volume 12106 of *Lecture Notes in Computer Science*, pages 280–310. Springer, 2020. doi:10.1007/978-3-030-45724-2_10.
9. Samuel Jaques, Michael Naehrig, Martin Roetteler, and Fernando Virdia. Implementing grover oracles for quantum key search on AES and lowmc. In Anne Canteaut and Yuval Ishai, editors, *Advances in Cryptology - EUROCRYPT 2020 - 39th Annual International Conference on the Theory and Applications of Cryptographic Techniques, Zagreb, Croatia, May 10-14, 2020, Proceedings, Part II*, volume 12106 of *Lecture Notes in Computer Science*, pages 280–310. Springer, 2020. doi:10.1007/978-3-030-45724-2_10.
10. Marc Kaplan, Gaëtan Leurent, Anthony Leverrier, and María Naya-Plasencia. Breaking symmetric cryptosystems using quantum period finding. In Matthew Robshaw and Jonathan Katz, editors, *Advances in Cryptology - CRYPTO 2016 - 36th Annual International Cryptology Conference, Santa Barbara, CA, USA, August 14-18, 2016, Proceedings, Part II*, volume 9815 of *Lecture Notes in Computer Science*, pages 207–237. Springer, 2016. doi:10.1007/978-3-662-53008-5_8.
11. Marc Kaplan, Gaëtan Leurent, Anthony Leverrier, and María Naya-Plasencia. Quantum differential and linear cryptanalysis. *IACR Trans. Symmetric Cryptol.*, 2016(1):71–94, 2016. doi:10.13154/tosc.v2016.i1.71-94.
12. Brandon Langenberg, Hai Pham, and Rainer Steinwandt. Reducing the cost of implementing AES as a quantum circuit, 2019.
13. Norbert Matthias Linke, Dmitri Maslov, Martin Roetteler, Shantanu Debnath, Caroline Figgatt, Kevin A. Landsman, Kenneth Wright, and Christopher R. Monroe. Experimental comparison of two quantum computing architectures. *Proc. Natl. Acad. Sci. USA*, 114(13):3305–3310, 2017. doi:10.1073/pnas.1618020114.
14. Seth Lloyd, Jeffrey H. Shapiro, Franco N. C. Wong, Prem Kumar, Selim M. Shahriar, and Horace P. Yuen. Infrastructure for the quantum internet. *Computer Communication Review*, 34(5):9–20, 2004. doi:10.1145/1039111.1039118.
15. Michael A. Nielsen and Isaac L. Chuang. *Quantum Computation and Quantum Information (10th Anniversary edition)*. Cambridge University Press, 2016. URL: <https://www.cambridge.org/de/academic/subjects/physics/quantum-physics-quantum-information-and-quantum-computation/>

quantum-computation-and-quantum-information-10th-anniversary-edition?
format=HB.

16. Thomas Santoli and Christian Schaffner. Using simon's algorithm to attack symmetric-key cryptographic primitives. *Quantum Inf. Comput.*, 17(1&2):65–78, 2017. URL: <http://www.rintonpress.com/xxqic17/qic-17-12/0065-0078.pdf>.
17. Vivek V. Shende, Aditya K. Prasad, Igor L. Markov, and John P. Hayes. Synthesis of reversible logic circuits. *IEEE Trans. on CAD of Integrated Circuits and Systems*, 22(6):710–722, 2003. doi:10.1109/TCAD.2003.811448.